A Novel Projection based Electro-Stereolithography (PES) Process for Composite Printing

Yayue Pan[1]*, Abhishek Patil[1], Chi Zhou[2]

1 Department of Mechanical and Industrial Engineering, University of Illinois at Chicago, Chicago, IL 60607

2 Department of Industrial and Systems Engineering, University at Buffalo, Buffalo, NY 14260

* Corresponding author: yayuepan@uic.edu, (312)996-8777

REVIEWED

ABSTRACT

Most current additive manufacturing processes can only process one material in one build. Few of them are able to fabricate multiple materials and composites, with limited choices of materials. In this research, we propose a novel Projection based Electro-Stereolithography (PES) process, which is able to fabricate composites with high resolution and fast speed, and a big range of material choices. The proposed novel additive manufacturing process integrates projection-based stereolithography and electrophotography approaches by using a photoconductive film and digital micro-mirror device (DMD). In PES, a photoconductive film is used to collect charged particles in the regions illuminated by light. More specifically, a laser beam is scanning on the film to create a latent image on the film and then a layer of charged particles is attracted to the illuminated area. A liquid bridge system and a stamping system have been developed to transfer particles from the film to liquid resin precisely. Furthermore, a digital mask is used to pattern the light irradiation of the DMD chip to selectively cure the photopolymer liquid resin and particles of that layer. By transferring particles with designed patterns to the resin in a projection based stereolithography system, we will be able to fabricate composites with various materials at microscopic resolutions very quickly. Challenges in this novel manufacturing process, including transferring of particles and curing control, have been discussed and addressed. The corresponding key parameters of the particles collecting, dropping and curing in the PES system have been identified. A proof-of-concept PES testbed has been developed and a couple of tests have been performed to validate the feasibility of the proposed additive manufacturing approach.

Keywords: multi-material printing, metal-polymer composite, additive manufacturing, electrophotography, stereolithography, vat photopolymerization.

1. INTRODUCTION

Additive Manufacturing (AM), which is also known as 3D printing or solid freeform fabrication, is a class of technologies that builds parts layer by layer using digital 3D design data[1]. In past decades, intensive research attempts have been made to improve its manufacturing capability, in terms of speed [2, 3], surface quality [4-6], material property[7-9], process reliability [8], etc. Compared to traditional manufacturing technologies, AM offers many unique advantages in terms of material\energy efficiency, simple operating style, more design flexibility, and so on[10]. Many industries have adopted AM in fabricating plastic or metal parts for various applications. However, the adoption of AM technologies as a means for fabricating

end-use components is still limited by the lack of AM materials. Material choices suitable for AM are far more limited than with traditional manufacturing processes[11].

In order to expand material selections, a few of composite AM technologies have been developed recently. For example, commercial machines like the Objet Connex 3D printer from Stratasys and ProJet 5500 from 3D Systems have recently entered into the market with the capability of printing multiple photopolymers in one build. By combining two base materials in specific concentrations and structures, as many as 14 different material can be created in a single printed part[12].

Yet these commercial machines only accept liquid photopolymers and the selection of materials are constrained by their flow ability in inkjet printer head. In addition to inkjet printing technique, some other research attempts have been made by investigating different AM techniques. Khalil et al. [13] presented a multi-nozzle deposition system for producing 3D tissue-engineered scaffolds. Chi et al.[14] developed a multi-material mask-image-projection-based stereolithography system, which could handle any liquid photopolymer. In addition to polymer, some research groups investigated selective laser sintering for multi-metallic-materials fabrication [15-18].

However, all those multi-material AM technologies are limited to one class of materials (polymer or metal). Very few of techniques based on stereolithography could process a mixture of metallic/polymer particles and liquid [19-21]. Yet the dispersion patterns of materials cannot be controlled.

To close the gap of multi-classes material additive manufacturing with controlled dispersion patterns, we propose a projection based electro-stereolithography (PES) approach in this paper, which has a potential to print multi-classes materials with controlled dispersion patterns. In particular, the thrust of this research is to study the feasibility of processing multi-classes liquid-particle materials in one build by integrating the fundamental principles of electrophotography and projection stereolithography. With the success of this process, the selection of materials in AM could be expanded significantly.

2. PROCESS DESCRIPTION

The novel additive manufacturing process we are developing in this research integrates projection-based stereolithography and electrophotography approaches, hence naming as Projection based Electro-Stereolithography (PES). The design of PES system and the relative methodologies are described in the coming sections.

2.1 Overview of PES Process

The PES process involves the additive manufacturing of a composite layer using two processes, projection based stereolithography and electrostatic deposition, and uses a photo curable resin and metal/polymer particles.

Projection stereolithography and electrophotography are mature technologies in 2D and 3D printing industries respectively. Projection based Stereolithography has been shown to offer high

material resolution, dimensional accuracy and good surface quality. By using a DLP projector and liquid photo curable resin, we can define and control the pattern of the images that will be projected on a surface area and in turn, the shape of the cured layer.

The electrophotography technology has achieved a high level of productivity and maturity in mainstream 2D printing but has very limited application in AM [22]. As the electrophotography based laser printing has substantially higher productivity, reliability and less cost than jetting based printing, the European consortium has been investigating large effort to overcome inherent challenges of multilayer printing by electrophotography to enable its use in mainstream AM [22]. However, the majority of the pioneer work is done by incorporating electrophotography into a powder bed fusion system, which suffers from the limited built height problem [22-25]. The proposed PES approach opens up exciting new ways of material distributions and processing in AM systems by incorporating electrostatic deposition mechanism into stereolithography based AM process. In the proposed PES system, heterogonous components and functional gradient materials are able to be manufactured through electrostatic depositions of materials such as polymer, metal, ceramic, and composite particles and photo-curing process.

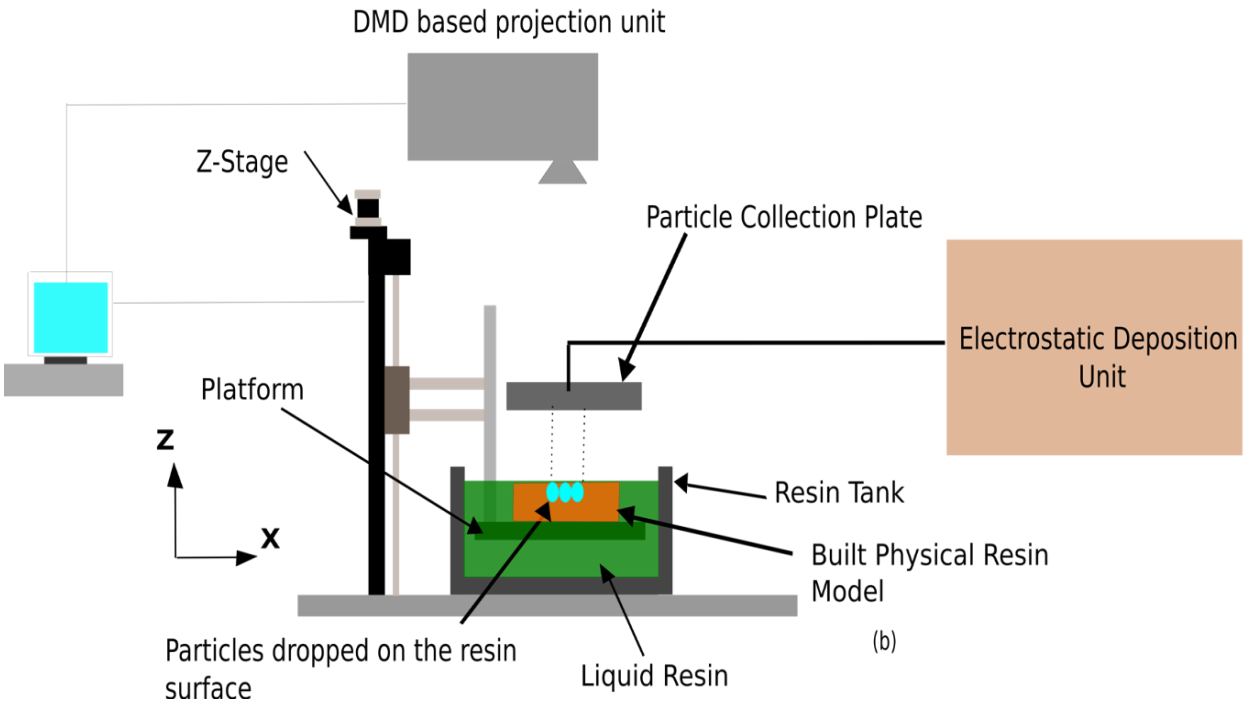

Figure 1: Illustration of Projection based Electro-Stereolithography (PES) process

The configuration of PES system is shown in Figure 1 and the process follows main seven steps:

(1) Initialization: Load the 3D digital model, slice the model into two sets of 2D images one for liquid resin photo-curing (Image set L) and other for particle patterning (Image set P), then move the platform and the particle collecting plate to home positions, turn on the projection unit and electrostatic deposition unit.
(2) Curing: Shine the 2D image of that layer from Image set L in the photo-curing set, to selectively cure the resin of that layer.

(3) Charging: In the electrostatic deposition unit, negatively sensitize the photoconductor surface with electrostatic charging by means of a corona charging device or charging roller for the toner cartridge.
(4) Exposing: In the electrostatic deposition unit, expose the photoconducting drum surface to the laser beam scanner to discharge the photoconductor and form the latent image according to the input 2D image (from Image set P) in the electrostatic deposition set.
(5) Particle collecting: In the electrostatic deposition unit, transfer the developed image to the particle collection plate. The charging roller positively charges the plate and the electrostatic force attracts the toner powder to jump on to the plate.
(6) Particle transferring: The plate that has particles on its surface is moved to the surface of liquid resin by linear stages. If it is desired to deposit particles on the cured resin, an elastomeric stamping method will be used to transfer particles. If it is desired to deposit particles on the liquid surface, a liquid bridge will be developed between the plate and the liquid resin, and then particles will be transferred to liquid resin along with the rupture of liquid bridge.
(7) 2nd-Curing: Shine the 2D image of that layer from Image set P, to fuse the newly transferred particles of that layer.

2.2 Hardware Components

The PES system design is depicted in Figure 2. To reduce the prototype cost and simplify the system design, an off-the-shelf projector (Acer H6510BD) is used as the projection device in the prototype system. The projector was fitted above the resin tank to give top-down projection. Various projection settings including focus, key stone rectification, brightness and contrast were adjusted to achieve a sharp projection image on the designed projection plane. The DMD resolution in our system is 1024×768 and the envelope size is set at $\mathbf{5.35 \times 4.06}$ inches. Three precise linear motion stages from Oriental Motor U.S.A. Co. (Elk Grove Village, IL) are used as the elevator for driving the platform and the particle collecting plate.

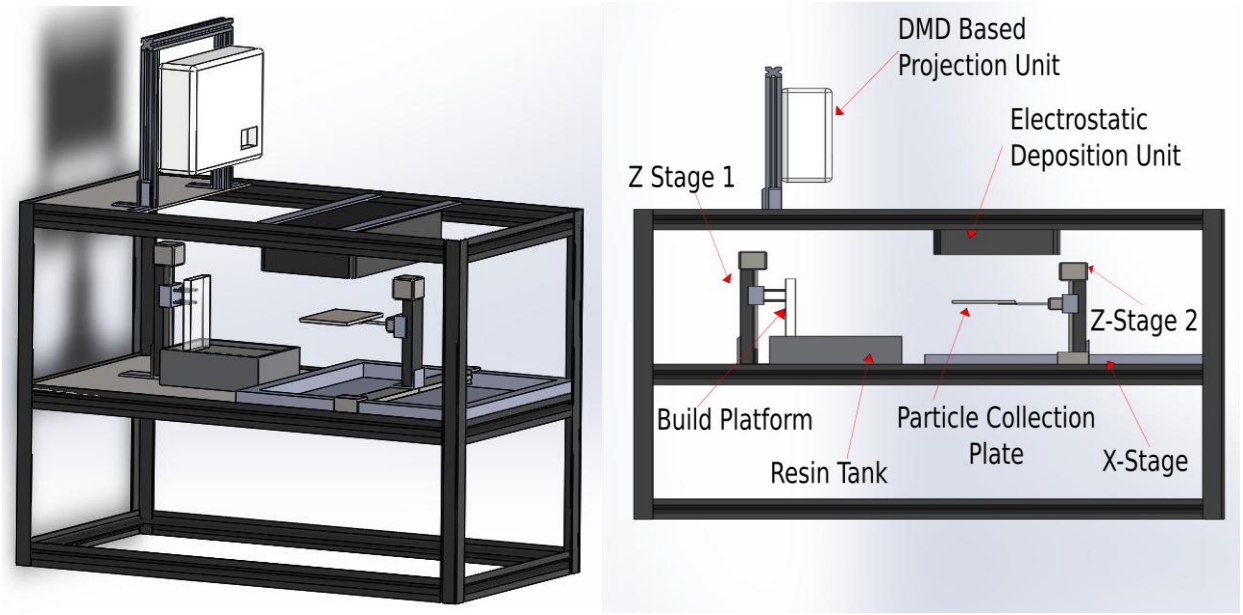

Figure 2: CAD model of the prototype hardware system for PES process

One is used as the Z elevator for lifting the build platform; another two are used as the stages for collecting particles from the electrostatic deposition unit and transferring particles to the liquid resin. A high performance 4-axis motion control board with 28 Bi-directional I/O pins from Dynomotion Inc. (Calabasas, CA) is used for driving the linear stages. Commercially available photocurable resin (envisonTEC Perfactory LS600M, Ferndale, MI) was used in the experiments. The electrostatic deposition unit was built from the parts of HP LaserJet (P1102w) printer.

2.3 Software System Components

A mask image planning test bed has been developed using the C++ language. It integrates the geometry slicing, digital mask generation, image loading, projection and motion controlling. Digital masks are constructed according to the material distribution of the sliced layer. Mask image projection is synchronized with the stage movement. The flow chart of the PES process and the graphical user interface (GUI) of the test bed is shown in Figure 3.

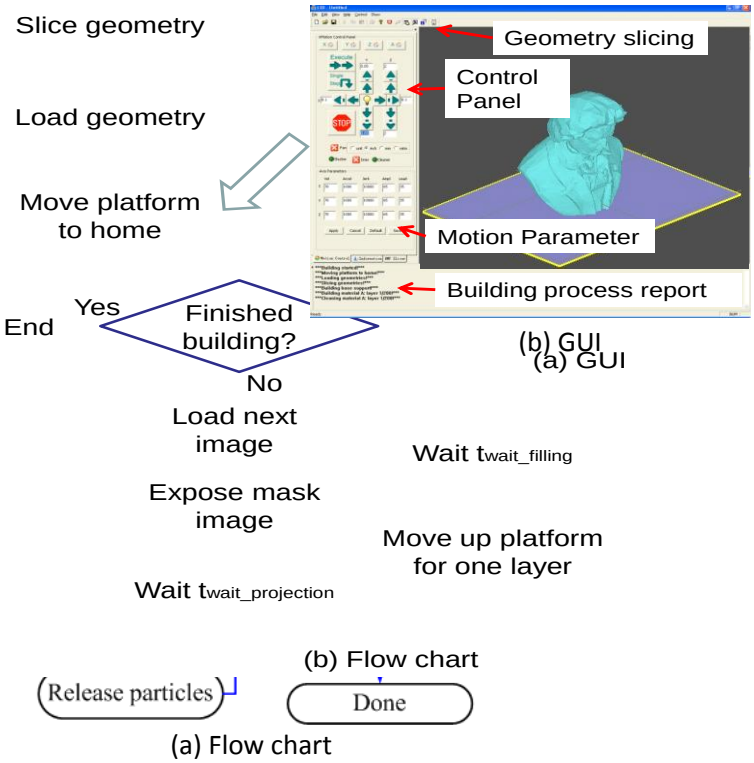

Figure 3: Graphical user interface (GUI) of the developed software system

3. PHYSICAL MODELING OF MATERIAL DEPOSITION AND CURING

3.1 Collecting Particles

The technology we are using for collecting the particles on the photo electrode is electrophotographic printing. Electrophotographic printing is a well-established and commonly used process in 2D laser printers where toner is selectively deposited onto a piece of paper to produce the desired printed copy.

The figure 4 shows an illustration of a typical electrophotographic printing process. The photoconducting drum is charged using corona discharging or direct contact charging methods. Here we have shown that the photoconducting surface of the drum is charged by corona discharge. This charged photoconducting surface is next exposed to a UV laser beam so that the charge on the surface is conducted away to the ground. Due to the electrostatic forces the charged particles dropped from the image developer adhere to the surface when it is brought in vicinity of the latent image. This image is then transferred on to the photoelectrode with the help of electric field. Thus the charged particles are collected on the photoelectrode surface. Lastly the photoconducting surface is cleaned by means of belt cleaning device before the process is repeated.

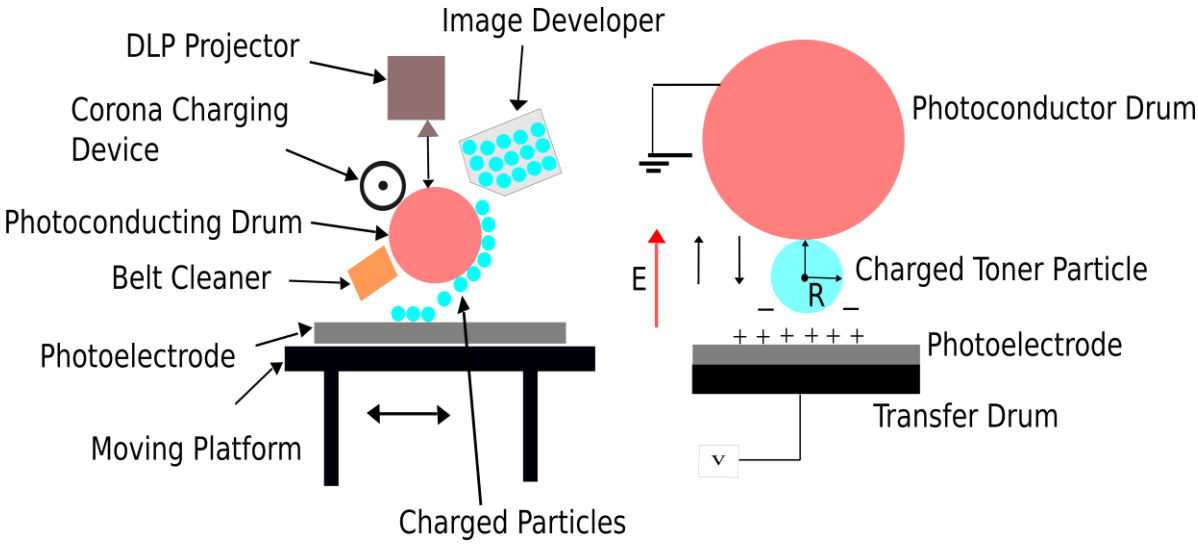

Figure 4: (a) Schematic Illustration of the Electrophotographic printing, (b) Force Model for the Toner-Photoelectrode arrangement.

The relationship between electric field intensity and the potential applied to the build platform is computed using Gauss Law's as follow[26, 27]. According to the special conditions in PES process, a simplified model of electric field could be derived as:

$$E\left(\frac{p}{\sigma_S}\right) = \frac{V_{DC}+\frac{\rho_1 {d_1}^2}{2K_1\epsilon_0}-\frac{\rho_2 {d_2}^2}{2K_2\epsilon_0}+\frac{p}{\epsilon_0}(\sigma_s+\rho_1 d_1)}{K_1\left(\frac{d_1}{K_1}+\frac{d_2}{K_2}+p\right)} \quad (1)$$

In the above equation, V_{DC} is the voltage applied across the build platform, p is the height of the printed part (or previously printed layers), d_1 is the thickness of the printed powder layer, d_2 is the thickness of the photoconducting drum layer, K_1, K_2 is the relative permittivity of the printed powder layer and the photoconductive drum layer respectively. ρ_1, ρ_2 denote the charge per unit volume in the fresh printed layer and photoconductive drum layer respectively. σ_s is the charge per unit area deposited on the print surface and ϵ_0 is the permittivity of the air.

Now the electrostatic detachment force F_E exerted on a spherical particle having a radius R and charge q from the photoconductor by an applied field of magnitude E is given by[28, 29]:

$$F_E = \beta qE - 4\lambda\pi\epsilon_0 R^2 E^2 \quad (2)$$

But in actual scenario a toner particle is partially surrounded by air and partially is in contact with the photoconductor surface. For these conditions it is not possible to draw a Gaussian surface around the particle, so the part of the toner particle, which is closest to the photoconductor surface, will have the greatest effect on the electrostatic attraction [28]. Within these approximations and that the dielectrics of the two materials are comparable equation (2) would reduce to:

$$F_E = qE \quad (3)$$

Also the toner particles are held to the photoconductor surfaces by two forces. The first is an electrostatic force F_1 caused by the toner particle inducing image charge within the photoconductor and is given by [28, 29]

$$F_I = -\beta \frac{q^2}{4\pi\epsilon_0 (2R)^2} \quad (4)$$

The second force is F_s arises from the surface forces such as those due to van der Waal's attraction. This force is given by the Johnson-Kendall-Roberts (JKR) equation[28, 30]:

$$F_s = -\frac{3}{2}\omega_A \quad (5)$$

where ω_A is the thermodynamic work of adhesion which is related to the surface free energies of the toner particle Υ_T and photoconductor Υ_S, as well as the interfacial energy by Υ_{TS}[28]

$$\omega_A = \Upsilon_T + \Upsilon_S + \Upsilon_{TS} \quad (6)$$

The approximate value of ω_A for a toner particle on an organic substrate is $\omega_A \sim 0.05\ \mathrm{J/m^2}$[31]. The force acting on the toner particle due to gravity F_W can be represented as

$$F_W = mg = pVg \quad (7)$$

So the net force F_T acting on the toner to separate the toner from the photoconductor surface should be greater than zero for successful deposition of the toner particles on the photoelectrode surface. From equations (3), (4), (5) and (6)

$$\mathrm{F_T = qE + \rho VG - [F_I + F_S + F_A] > 0} \quad (8)$$

Here F_A is including all the adhesion and cohesion forces, other than Van Der Waals, double layer, chemical, hydrophobic etc. [32].

Considering the toner particle size, mass, density and volume for this experiment it might appear that the effect of the surface forces and force on toner particles due to gravity may be minute and can be neglected. Moreover the surface force could be easily be balanced by another

surface force if the toner particle is further in contact with another surface apart from photoconductor surface like the another toner particle[28]. Thus the net force required to detach the toner particle from the photoconductor drum would reduce to

$$F_T = qE - F_I > 0 \quad (9)$$

Also by decreasing the air gap and the toner particle to photoconductor adhesion, we can significantly increase the rate and ease of transfer.

A test bed was designed and developed in order to explore the electrophotographic printing process and to determine what kind of materials could be used to electrostatically charge and transfer to the build platform.

3.2 Particles Transfer Mechanism

3.2.1 Liquid Bridge Approach

After collecting particles in the desired areas of the particle collection plate, the plate is turned over and then moved down until it touches the surface of liquid resin in the vat. After waiting for a few seconds, the plate is lifted up slowly from the liquid. Initially, a small gap is formed between the plate and the liquid surface, leading to a liquid bridge. As the plate moves up, the liquid bridge finally breaks and then particles fall into the liquid together with the rupture of the liquid bridge.

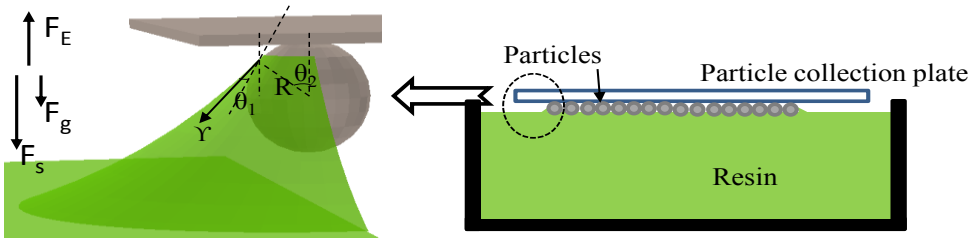

Figure 5: Schematic illustration of the particle transfer process through liquid bridge.

Here we consider the pull-off force exerted on a spherical particle, as shown in Figure 5. The pull-off force consists of the vertical component of liquid bridge force F_s and gravity force F_g. The adhesion force exerted on the particle is mainly from the electrostatic force F_E. The dynamics and rupture conditions of liquid bridges are widely studied [33-39]. The vertical component of liquid bridge force is typically modeled by analyzing the total free energy of liquid bridge[34]:

$$F_s = \sigma \cdot l_t \cdot \sin(\theta_2 - \theta_1) + \Delta P \cdot A \quad (10)$$

where σ is the surface tension, ΔP is the difference between vapor pressure and liquid pressure, θ_1 is the contact angle, θ_2 is the deviation angle and l_t is the perimeter of the interfacial area A. The geometric relationships of these parameters are shown in Figure 6. This is a 3D problem and there are numerous particles on the flat plate. Before the liquid bridge breaks, it could be considered that the outside half of the particle forms the liquid/air/solid interfaces and the inside

half of the particle is immersed within the liquid. Therefore the interfacial parameters could be approximated as:

$$l_t = \pi R \sin\theta_2 \tag{11}$$

$$A = \pi(R \sin\theta_2)^2 \tag{12}$$

$$\Delta P = \frac{2\sigma}{r_m} \tag{13}$$

where R is the radius of the particle, and r_m is the mean radii of the liquid interfacial profile. Substituting equation (11) (12) (13) into (10) leads to:

$$F_s = \sigma\pi R \sin\theta_2 \,(\sin\theta_1 + \frac{2r}{r_m}) \tag{14}$$

The gravity component is:

$$F_g = \frac{4}{3}\pi R^3 \rho_P g \tag{15}$$

Therefore, in order to drop particles to the liquid resin, the following condition should be satisfied:

$$F_s + F_g > F_E \tag{16}$$

Substituting (11), (13), (15) and (16) into (17) leads to:

$$\sigma \cdot l_t \cdot \sin(\theta_2 - \theta_1) + \Delta P \cdot [\,\pi(R \sin\theta_2)^2 + \frac{4}{3}\pi R^3 \rho_P g > F_E \tag{17}$$

3.2.2 Elastomeric Stamp Approach

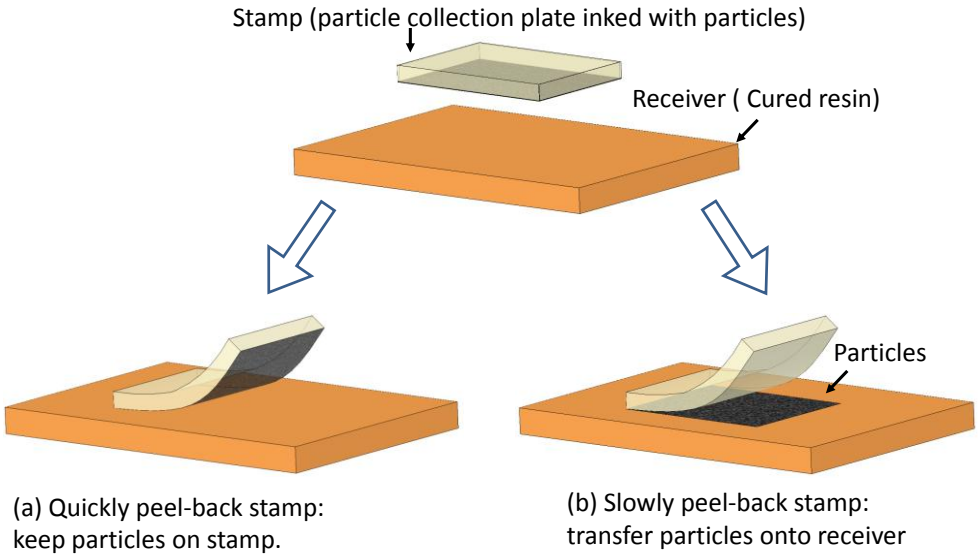

Figure 6. An illustration of the particle transfer process through elastomeric stamp

Another approach to release particles is to transfer particles on cured resin surface using elastomeric stamp transfer mechanism. The stamp transfer technology is widely used in printing objects with a wide range of sizes and shapes, onto a variety of substrates without specially designed surface chemistries or separate adhesive layers[40].

As shown in Figure 6, the particle collection plate is composed of a Teflon film on a PDMS substrate. It is working as a soft elastomeric stamp inked with particles. And the cured resin surface is served as a receiving substrate. Contacting the soft elastomeric plate against the cured resin surface leads to a conformal contact, driven by van der waals interaction dominated adhesion forces [41, 42]. According to Rogers et. al. study[40], the adhesion between the elastomeric surface and the solid surface is rate-sensitive owing to the viscoelastic behavior of the elastomer. In turn, the particle transfer mode is dependent on the velocity used to pull the elastomeric surface away. In order to release particles from the elastomeric plate to the cured resin surface, the plate should be brought into contact with the resin surface, and then be removed with sufficiently low velocity. With a sufficiently low velocity (~1mm/s), the particles could adhere preferentially to the cured resin surface and separate from the plate.

4. CASE STUDY OF HETEROGENEOUS COMPOSITE PRINTING

Three test cases have been performed to study the feasibility of the PES process for composite printing. Various parameters like weight ratio, curing time and model dimensions were considered to successfully execute the test experiments. The liquid resin used for this study is a commercial photopolymer (envisonTEC Perfactory LS600M). The test particles used for this preliminary study were the toner particles of the HP LaserJet P1102w printer. Different patterns of the particles dropping on the resin surface were studied and the results are discussed in the following sections.

4.1 Test of photo-curing components

To make sure the proposed PES process and developed prototype system have no issues in its photo-curing part, two sample test cases were conducted. The manufacturing capability of the fabricating parts with pure resin was verified by first fabricating a spur gear and then a cube array. The photo-curing area is set at 135.80×103.124 mm.

This fabricated model constitutes 122 layers in total, including 3 base layers with each layer thickness corresponding to 152.3 μm. Initial exposure time for the base layer was 150 seconds (2.5 minutes) per layer whereas for the subsequent layer it was 15 seconds each. Sleeping time of 3 seconds was introduced when the stage goes down inside the resin tank to provide enough time for the fresh resin to uniformly cover the top layer of the part with fresh resin in the tank. The entire building process was completed in 47 minutes, which also includes settling time of 21 seconds per layer. Since a top-down projection has been adopted, after each layer the platform travels down a certain distance (~ 2.5mm) and then while retracting it up to coat one layer of liquid on its top. The gear design and fabricated parts are shown in Figure 7 (a) and (b).

The second test case for photo-curing process validation is a cube array as shown in Figure 7 (c) and (d). This model is sliced into 14 layers in total, 0 images in image set P and 14 images in

image set L. A bigger layer thickness of 203.2 μm is used for this test. The cube array as shown in the Figure 10 is 38×38 mm and has a thickness of 2.84 mm.

These two simple tests showed that the mask image planning, light projection and liquid curing components are working properly in the developed PES system, and it is ready to receive particles for composite manufacturing.

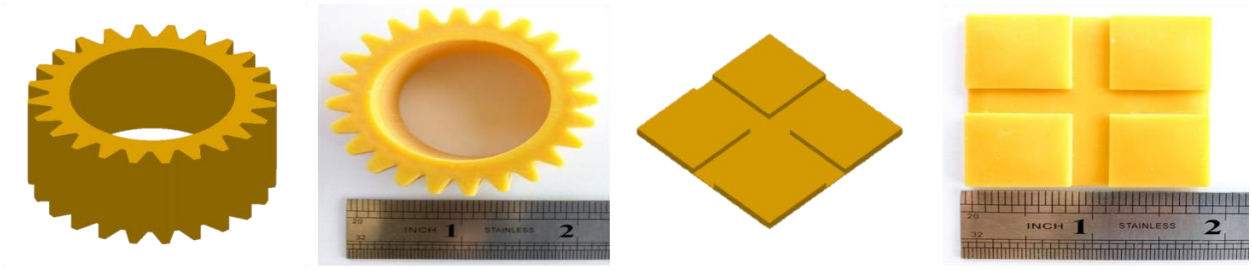

(a) (b) (c) (d)

Figure 7 - (a) CAD model of spur gear; (b) fabricated gear; (c) CAD model of cube array, (d) fabricated cube array

4.2 Resin + Particles Photo-Curing Test

Because our electrostatic unit was developed from a modified off-the-shelf 2D laser printer, the material-machine interactions in the electrostatic deposition process are not known yet. To eliminate the influence of unknown material properties on PES process performance, we use the original toner cartridge particles to test the particle dropping and particle-resin curing components in the developed PES system.

4.2.1 Test of Lateral Distribution of Particles with Designed Pattern

A cube array with particles forming "UIC" letters on its top left surface is tested to validate the capability of PES technology in selectively distributing particles on a lateral plane.

Its CAD model and the fabricated part are shown in Figure 8. The model is sliced to 15 layers, generating 15 mask images in Image set L named "L_1, L_2 till L_15", and one mask image in Image set P named P_14. Image P_14 includes digital information of the "UIC" pattern for particles deposition and curing.

From layer #1 till layer #14, the part was built layer-by-layer using mask images in set L. After finishing the 14th layer, the image P_14 was the input image and the laser scanned the photoconductive surface to form a latent image on the photoconductor surface. The toner particles were deposited on the particle collection plate due to the electrostatic force. Then the elastomeric stamping approach is used to transfer particles to the surface of the cured 14^{th} layer.

After this, the image P_14 is exposed directly on the particles to improve the bonding between particles and cured resin surface. The exposure time is about 20 seconds. After the 2nd curing step, the stage would go inside the tank to recoat a fresh resin layer for 15th layer curing.

To demonstrate the particles distribution pattern, two parts were fabricated. One part was fabricated by stopping the building process at 14^{th} layer, so that the 15^{th} layer of resin does not

cover the particles. Figure 8 (b) shows the fabricated part without the 15th layer. Figure 8 (c) is the microscopic image of the blue-circled area in (b). It shows particles on the 14th layer. From (b) and (c), we can observe that the majority of particles have been transferred successfully from collection plate to resin surface. The "UIC" pattern formed by electrostatic deposition process is retained pretty well after the transfer.

Another part is fabricated by completing the 15th layer. So the UIC patterned particles are hidden below the top layer. Figure 8 (d) is the microscopic image of the same blue-circled area in this part, which has a layer of cured resin covering the particles. Because the top layer resin is only 203μm thick, the particles beneath are still visible, as showed in (d).

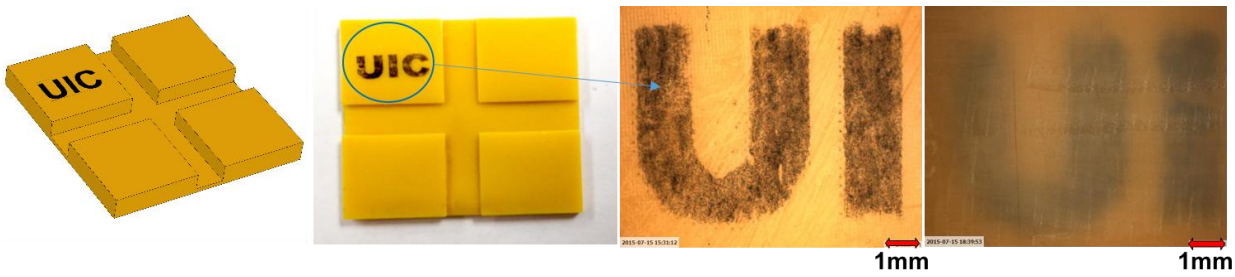

Figure 8 – (a) CAD model, (b) fabricated cube array part without 15th layer, (c) microscopic images- top view of particles, and (d) microscopic image- top view of particles after 15th layer

4.2.2 Test of Vertical Particle Distribution Pattern Control

A cuboidal model is used to test the capability of PES technology in selectively distributing particles in vertical direction with designed patterns. The toner particles (black color) were imprinted on the 42nd and 46th layer of the 50 layers of the build part. The same manufacturing process as described in section 3 with parameter settings are used.

The CAD model and the fabricated part are shown in Figure 9 (a), (b) and (c). The model is sliced to 50 layers, generating 50 mask images in Image set L named "L_1, L_2 till L_50", and two mask images in Image set P named P_42 and P_46. These images include digital information of the designed horizontal pattern for particles deposition and curing.

From layer #1 till layer #41, the part was built layer-by-layer using mask images in set L. After finishing the 41st layer, the image P_42 was input and the laser scanned the photoconductive surface to form a latent image on the photoconductor surface. The toner particles were deposited on the particle collection plate due to the electrostatic force. Then the elastomeric stamping approach is used to transfer particles to the desired area on the surface of the cured 41st layer.

After this, the image P_41 is exposed directly on the particles to improve the bonding between particles and cured resin surface. The exposure time is about 20 seconds. After the 2nd curing step, the stage would go inside the tank to recoat a fresh resin layer for 42nd layer curing. Then again mask images in set L are exposed till layer# 45, image P_46 was the input to form a latent image on the photoconductor surface and transferred to the desired area on the surface of the cured 45th layer.

Figure 9 (d) and (e) are the microscopic images of the part. It is shown that particles are distributed in designed layers. From the figure the color distribution is very clear and even, such that we can distinctly differentiate between two particle layers from the actual and microscopic images.

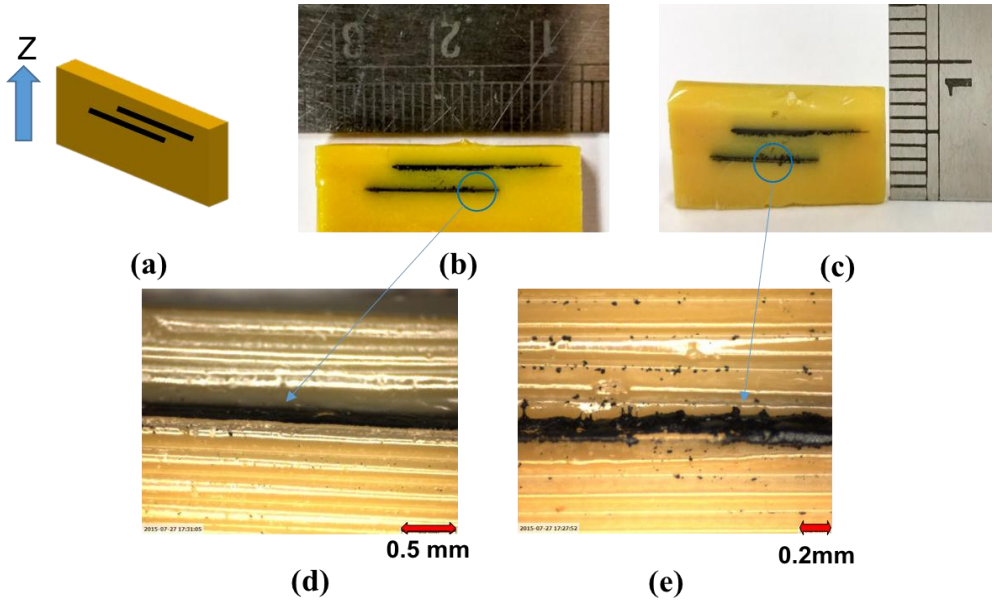

Figure 9 – (a) CAD model, (b) top view of the fabricated model with toner particles in 42nd and 46th layer out of the 50 layers of the part, (c) side view of the fabricated part (d) microscopic image of test case 1- side view of the fabricated part where we can distinguish between particle-resin layers, and (e) microscopic image of test case 2- side view of the fabricated part

5. CONCLUSION AND FUTURE WORK

A novel additive manufacturing technology, Projection Electro-Stereolithography(PES), is developed in this paper for multi-material/composite printing. PES process uses electrostatic deposition principle to collect particles in a plate layer by layer, and then uses liquid bridge method or elastomeric stamping method to transfer particles to resin vat, hence is able to distribute particles into photopolymer layer by layer, with controlled patterns. Compared to existing multi-material printing approach in Stereolithography related AM systems, which usually mix particles with liquid resin evenly first and then use the paste as raw material, PES has a unique advantage in controlling the embedding patterns of particles precisely. This unique characteristic could potentially open a new avenue for advanced composite materials design and additive manufacturing functional products.

Feasibility and challenges in implementing this new technology are discussed in this paper. First, collection of one layer of particles each time avoids the historical research problems in applying 2D electrophotography technique into 3D printing. Secondly, transferring of particles with well-kept patterns is investigated, and liquid bridge method and elastomeric method have been developed for different conditions. Accordingly, a proof-of-concept test bed has been developed. Case studies have been performed to verify the capability of this new process on building composites with designed particle embedding patterns. The effectiveness of the PES

process for embedding particles into polymer matrix with different distribution patterns in a three dimension has been demonstrated. Yet challenges also found, like holding particles on place during resin recoating process.

As a new manufacturing technology, considerable work remains to mature the process and the related prototype system to overcome current challenges and improve its performance. Some on-going investigations in our group include:

- Testing other particles for electrostatic depositing and transferring.
- Investigating other approaches for improving the bonding between particles and cured resin, like thermal fusing.
- Testing new collection plate coating materials to form proper liquid bridges for dropping particles directly on liquid resin surface without disturbing its pattern.

REFERENCES

1. Wong, K.V. and A. Hernandez, *A review of additive manufacturing.* ISRN Mechanical Engineering, 2012. **2012**.
2. Ha, Y.M., J.W. Choi, and S.H. Lee, *Mass production of 3-D microstructures using projection microstereolithography.* Journal of mechanical science and technology, 2008. **22**(3): p. 514-521.
3. Pan, Y.Y., C. Zhou, and Y. Chen, *A Fast Mask Projection Stereolithography Process for Fabricating Digital Models in Minutes.* Journal of Manufacturing Science and Engineering-Transactions of the Asme, 2012. **134**(5).
4. Pan, Y. and Y. Chen, *Smooth Surface Fabrication based on Controlled Meniscus and Cure Depth in Micro-Stereolithography.* 2015.
5. Pan, Y., et al., *Smooth surface fabrication in mask projection based stereolithography.* Journal of Manufacturing Processes, 2012. **14**(4): p. 460-470.
6. Sun, C., et al., *Projection micro-stereolithography using digital micro-mirror dynamic mask.* Sensors and Actuators a-Physical, 2005. **121**(1): p. 113-120.
7. Pan, Y., et al., *Multitool and Multi-Axis Computer Numerically Controlled Accumulation for Fabricating Conformal Features on Curved Surfaces.* Journal of Manufacturing Science and Engineering-Transactions of the Asme, 2014. **136**(3).
8. Turner, B.N., R. Strong, and S.A. Gold, *A review of melt extrusion additive manufacturing processes: I. Process design and modeling.* Rapid Prototyping Journal, 2014. **20**(3): p. 192-204.
9. Zhao, X.J., et al., *An integrated CNC accumulation system for automatic building-around-inserts.* Journal of Manufacturing Processes, 2013. **15**(4): p. 432-443.
10. Huang, S.H., et al., *Additive manufacturing and its societal impact: a literature review.* The International Journal of Advanced Manufacturing Technology, 2013. **67**(5-8): p. 1191-1203.
11. Berman, B., *3-D printing: The new industrial revolution.* Business Horizons, 2012. **55**(2): p. 155-162.
12. Materials, P.D. [cited 2015 7/15]; Available from: http://www.stratasys.com/materials/polyjet/digital-materials.
13. Khalil, S., J. Nam, and W. Sun, *Multi-nozzle deposition for construction of 3D biopolymer tissue scaffolds.* Rapid Prototyping Journal, 2005. **11**(1): p. 9-17.
14. Zhou, C., et al. *Development of Multi-Material Mask-Image-Projection-Based Stereolithography for the Fabrication of Digital Materials*. in *Annual Solid Freeform Fabrication Symposium, Austin, TX*. 2011.

15. Liew, C.L., et al., *Dual material rapid prototyping techniques for the development of biomedical devices. Part 2: Secondary powder deposition.* International Journal of Advanced Manufacturing Technology, 2002. **19**(9): p. 679-687.
16. Liew, C.L., et al., *Dual material rapid prototyping techniques for the development of biomedical devices. Part 1: Space creation.* International Journal of Advanced Manufacturing Technology, 2001. **18**(10): p. 717-723.
17. Jackson, B., K. Wood, and J. Beaman, *Discrete multi-material selective laser sintering (M 2 SLS): development for an application in complex sand casting core arrays.* Proc Solid Freeform Fabr, 2000. **2000**: p. 176-182.
18. Santosa, J., D. Jing, and S. Das, *Experimental and numerical study on the flow of fine powders from small-scale hoppers applied to SLS multi-material deposition–part I.* Ann Arbor, 2002. **1001**: p. 48109-2125.
19. Bartolo, P. and J. Gaspar, *Metal filled resin for stereolithography metal part.* CIRP Annals-Manufacturing Technology, 2008. **57**(1): p. 235-238.
20. Kumar, S. and J.-P. Kruth, *Composites by rapid prototyping technology.* Materials & Design, 2010. **31**(2): p. 850-856.
21. Wurm, G., et al., *Prospective study on cranioplasty with individual carbon fiber reinforced polymere (CFRP) implants produced by means of stereolithography.* Surgical neurology, 2004. **62**(6): p. 510-521.
22. Jones, J., et al. *Additive manufacturing by electrophotography: Challenges and successes*. in *NIP & Digital Fabrication Conference*. 2010. Society for Imaging Science and Technology.
23. Kumar, A.V., A. Dutta, and J.E. Fay, *Electrophotographic printing of part and binder powders.* Rapid Prototyping Journal, 2004. **10**(1): p. 7-13.
24. Kumar, A.V., A. Dutta, and J.E. Fay. *Solid freeform fabrication by electrophotographic printing*. in *14th Solid Freeform Fabrication symposium*. 2003.
25. Kumar, A.V. and A. Dutta, *Investigation of an electrophotography based rapid prototyping technology.* Rapid Prototyping Journal, 2003. **9**(2): p. 95-103.
26. Cross, J., *Electrostatics: principles, problems and applications.* 1987.
27. Kumar, A.V. and A. Dutta, *Electrophotographic layered manufacturing.* Journal of manufacturing science and engineering, 2004. **126**(3): p. 571-576.
28. Rimai, D., D. Weiss, and D. Quesnel, *Particle adhesion and removal in electrophotography.* Journal of adhesion science and technology, 2003. **17**(7): p. 917-942.
29. Rimai, D.S., S.o.P. Adhesion, and A. Society, *Advances in particle adhesion:[selected papers from the Symposium on Particle Adhesion at the 17th annual meeting of the Adhesion Society, Orlando, Florida, USA, February 21-23, 1994]*. 1996: Gordon & Breach.
30. Johnson, K., K. Kendall, and A. Roberts. *Surface energy and the contact of elastic solids*. in *Proceedings of the Royal Society of London A: Mathematical, Physical and Engineering Sciences*. 1971. The Royal Society.
31. Rimai, D. and D.J. Quesnel, *Fundamentals of particle adhesion*. 2001: Global Press.
32. AL-Rubaiey, H., *Toner Transfer and Fusing in Electrophotography.* Graphic Arts in Finland, 2010. **39**: p. 1.
33. Benilov, E.S. and C.P. Cummins, *The stability of a static liquid column pulled out of an infinite pool.* Physics of Fluids, 2013. **25**(11).
34. Gao, S., et al., *The Liquid-Bridge with Large Gap in Micro Structural Systems.* Journal of Modern Physics, 2011. **Vol.02No.05**: p. 12.
35. Knospe, C.R. and H. Haj-Hariri, *Capillary force actuators: Modeling, dynamics, and equilibria.* Mechatronics, 2012. **22**(3): p. 251-256.

36. Yang, L., Y. Tu, and H. Fang, *Modeling the rupture of a capillary liquid bridge between a sphere and plane.* Soft Matter, 2010. **6**(24): p. 6178-6182.
37. Bowden, N., S.R.J. Oliver, and G.M. Whitesides, *Mesoscale self-assembly: Capillary bonds and negative menisci.* Journal of Physical Chemistry B, 2000. **104**(12): p. 2714-2724.
38. Nosonovsky, M. and B. Bhushan, *Multiscale effects and capillary interactions in functional biomimetic surfaces for energy conversion and green engineering.* Philosophical Transactions of the Royal Society a-Mathematical Physical and Engineering Sciences, 2009. **367**(1893): p. 1511-1539.
39. Chen, H., T. Tang, and A. Amirfazli, *Liquid transfer mechanism between two surfaces and the role of contact angles.* Soft matter, 2014. **10**(15): p. 2503-2507.
40. Meitl, M.A., et al., *Transfer printing by kinetic control of adhesion to an elastomeric stamp.* Nature Materials, 2006. **5**(1): p. 33-38.
41. Hsia, K., et al., *Collapse of stamps for soft lithography due to interfacial adhesion.* Applied Physics Letters, 2005. **86**(15): p. 154106.
42. Huang, Y.Y., et al., *Stamp collapse in soft lithography.* Langmuir, 2005. **21**(17): p. 8058-8068.